

Design and Implementation of an Autonomous Robot for Steel Bridge Inspection

Nhan H. Pham and Hung M. La, *Senior Member, IEEE*

Abstract—Steel bridges constitute the second most bridges in the U.S. while the number of deficient bridges are growing. Currently, the majority number of current bridge inspections are done manually by inspectors which require significant amount of human resources along with expensive and specialized equipment. Moreover, it is difficult and dangerous for inspectors to inspect large bridges with high structures. In this paper, we propose a new design and implementation of a robotic system that can be used for steel bridge inspection. The robot consists of four magnetic wheels which create adhesion to steel surface. It is able to carry multiple sensors for navigation and mapping. Collected data are sent to the ground station for live monitoring as well as further processing. In addition, magnetic field and range sensors are also integrated to enable robot to move safely on steel surfaces. Results with physical tests on real steel structures are shown to validate the feasibility of robot design.

I. INTRODUCTION

A. Motivation

As the number of infrastructures especially bridges are growing which have recently passed 600,000 in the U.S [1]. Among more than 200,000 steel bridges, one third of them are either deficient or functionally obsolete which are likely a growing threat to human's safety. Collapse of numerous bridges recorded over past 15 years has shown significant impact on the safety of all travelers. In particular, the Minneapolis I-35W Bridge in Minnesota, U.S collapsed in 2007 due to undersized gusset plates, increased concrete surfacing load, and weight of construction supplies/equipment [2]. There was a recent report in 2013 related to Scott City roadway in Missouri, U.S collapsing two sections of the bridge onto the rail line. These accidents may result from inadequate bridge inspection and maintenance due to large number of bridges needed to be taken care of. Hence, there have been many research to apply advanced technology including robotics to assist human for bridge inspection and maintenance. However, those activities require great amount of human resources along with expensive and specialized equipment. Currently, most bridge inspections are done by inspectors with visual inspection or using manual methods such as hammer tapping and chain dragging for delamination and corrosion detection which are very time consuming. Moreover, it is really difficult and dangerous to inspect large bridges with high structures since inspectors have to

climb up very high or hang on cable to do inspection as shown in Fig. 1. In addition, reports from visual inspection may vary between inspectors, hence the bridge's condition cannot be assessed precisely. We can use a robotic system carrying several advanced evaluation sensors to climb on those bridges to collect data for condition assessment. It will significantly improve the inspection efficiency as well as enhance inspectors safety since they no longer have to work under dangerous conditions.



Fig. 1. Dangerous bridge inspection scenes, source: Harcon Corporation and Working AT Height Alti-Service™.

B. Literature Review

The number of research groups that apply advanced robotics technology in order to automatically inspect bridges is growing over the last two decades [3]–[5]. Devault [6] developed a robot that is able to inspect underwater bridge structures whereas others were working with bridge deck inspection robots [7], [8]. La et al. [9], [10] developed an autonomous robotic system integrated with advanced non-destructive evaluation (NDE) sensors for high-efficiency bridge deck inspection and evaluation. Li et al. [11] also utilized NDE technique to perform automatic inspection on bridge deck and record bridges health condition. In the other hand, there were several works focusing on cable inspection. Xu et al. introduced the design and experiments of a wheel-based cable inspection robotic system consisting of CCD cameras for visual inspection [12]. Similar robot [13] enables effective visual inspection of the cable on suspension bridge. Besides, there were studies that covered other bridge structures inspection. Oh et al. [14] introduced a robotic platform to manually or automatically inspect beneath the bridges by long-distance users with a 3-dimensional (3D) graphical user interface. Furthermore, there were several initial implementations of climbing robots for inspection in late 1990s [15], [16]. Mazumdar et al. [17] proposed a legged robot that moves across a steel structure for steel bridge inspection. Powerful permanent magnets imbedded in each foot allow the robot to hang from a steel ceiling powerlessly

This work is supported by the University of Nevada, Reno and the National Science Foundation under the grants: NSF-ICorps#1559942.

Nhan Pham and Hung La are with the Advanced Robotics and Automation (ARA) Lab, Department of Computer Science and Engineering, University of Nevada, Reno, NV 89557, USA. Corresponding author: Hung La, email: hla@unr.edu.

while the attractive force is modulated by tilting the foot against the steel surface. A robot with magnetic wheels was developed by Wang et al. [18] carrying Giant Magneto Resistive sensor array for crack and corrosion detection. Liu et al. also proposed a bridge inspection method using a wall-climbing robot based on negative pressure adhesion mechanism which collects crack images with a high-resolution camera so that the crack could be extracted and analyzed precisely [19], [20]. Taking advantage of attraction force created by permanent magnets, Leibbrandt et al. [21] and Leon-Rodriguez et al. [22] developed different wall-climbing robots carrying NDE devices to detect weld defects, cracks, corrosion testing that is capable of inspecting oil tanks or steel bridges. San-Millan [23] presented the development of a teleoperated wall climbing robot which can be equipped with various testing probes and cameras for different inspection tasks. Zhu et al. [24] used a magnetic wall-climbing robot capable of navigating on steel structures, measuring structural vibrations, processing measurement data and wirelessly communicating information to investigate field performance of flexure-based mobile sensing nodes (FMSNs). The FMSNs were deployed to identify minor structural damage, illustrating a high sensitivity in damage detection enabled by flexible mobile deployment.

In this paper, the design and implementation of a four-wheeled robot for steel bridge inspection is introduced. Taking advantage of adhesion force created by permanent magnets, the robot is able to move freely on steel surface, carry several sensors for visual crack detection and structure mapping, and wirelessly controlled. With an advanced mechanical design, the robot is able to carry a decent load (approximately 4kg) while climbing on both inclination and upside-down surfaces. The robot can also transition from one surface to another surface with up to 90 degrees change in orientation. Collected data are sent to a ground station in for real time monitoring and further processing. In addition, magnetic field sensors and range sensors are also integrated to help robot move safely on steel surfaces.

The rest of the paper is organized as follows. Section II describes the overall robot design. Section III illustrates the robots control. Section IV shows various experiments to verify robot design and section V gives the conclusion and future work.

II. OVERALL DESIGN

A. Mechanical Design

A four motorized wheels robot design is proposed which takes advantage of permanent magnets for adhesion force creation. Therefore, it allows the robot to adhere to steel surfaces without consuming any power. In addition, cylinder shaped magnets are used for convenience and flexibility in adjusting the attraction force. Moreover, eight high torque servo motors are modified to use for driving four wheels and four shafts which are used for robot lifting. The robots parameters are shown in Table I while motors parameters are listed in Table II.

TABLE I
ROBOT PARAMETERS

Length	220.9 mm
Width	130 mm
Height	241.26 mm
Weight	14 lbs. (without payload) and 20 lbs. (full load)
Drive	4 motorized wheels
Controller	Embedded controller + onboard computer

TABLE II
MOTOR PARAMETERS

Torque	525 g/mm (2S Li-Po)
Speed	0.12 sec/ 60 ^O (2S Li-Po)
Length	40.13 mm
Width	20.83 mm
Height	39.62 mm
Weight	71 g
Voltage	6-8.5V (2S Li-Po battery)

Each wheel contains slots which can be filled with up to 36 Neodymium magnet cylinders with poles on flat ends as shown in Fig. 2. This design gives us the flexibility in determining the amount of magnetic force and helps reduce the weight of the robot. According to on [25], if there is an air gap between magnet cylinders and steel frame, the pull force is greatly affected. Table III and Fig. 3 describe the relationship between magnetic pull force and the air gap. Additionally, four wheels are designed such that the robot can overcome several situations including transitioning from one surface to another surface with up to 90 degrees change in orientation or getting rid of being stuck. Additionally, four shafts have been added in order to lift either front or rear wheels off the ground if the robot is stuck on rough terrains as shown in Fig. 4.

From this wheel design, there are always either four or five magnet cylinders which are within 1mm from the steel surface as shown in Fig. 5. From Table III, the magnetic force created from each wheel can be calculated if 7/16" x 7/16" magnet cylinders are used is as following:

$$F_{mag_{i,i=1,\dots,4}} = 50.6 * 2 + 19.6 * 2 = 140.4(N)$$

or

$$F_{mag_{i,i=1,\dots,4}} = 50.6 + 19.6 * 4 = 129(N)$$

where $F_{mag_i} = \|\vec{F}_{mag_i}\|$ is the Euclidean norm of \vec{F}_{mag_i} .

TABLE III
PULL FORCE OVER AIR GAP (7/16" X 7/16" MAGNET)

Distance (mm)	PullForce (N)		
	Magnet to steel plate	Between two steel plates	Magnet to magnet
0	50.6	57.7	50.4
1	19.6	26.9	29.3
2	10.8	16.7	20.9
3	6.5	11.1	15.6
4	4.1	7.7	12
5	2.7	5.4	9.5
6	1.8	3.9	7.5
7	1.3	2.9	6.1
8	0.9	2.2	4.9
9	0.6	1.6	4
10	0.5	1.3	3.3

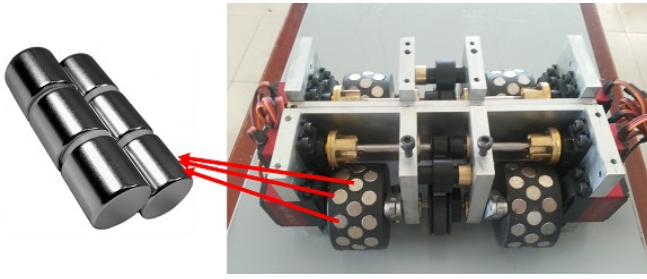


Fig. 2. Wheels with magnet cylinders.

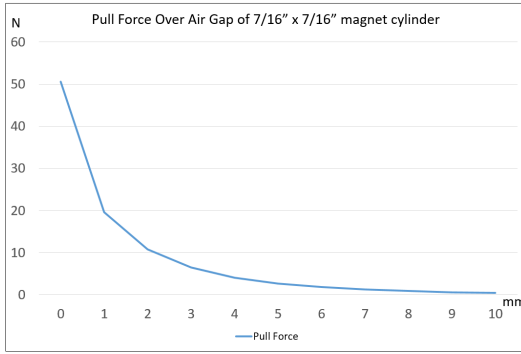


Fig. 3. Pull force over air gap of 7/16 x 7/16 magnet cylinder.

Therefore, the total magnetic force in theory can be at least: $\sum_{i=1}^4 (F_{mag_i}) \geq 129 * 4 = 516(N)$.

However, each wheel is covered with a 1mm layer of cloth to increase the friction with the steel surface. Therefore, the real magnetic force is calculated as:

$$F_{mag_{i,i=1,\dots,4}} = 19.6 * 2 + 10.8 * 2 = 60.8(N)$$

or

$$F_{mag_{i,i=1,\dots,4}} = 19.6 + 10.8 * 4 = 62.8(N).$$

Theoretically, the total magnetic force is at least:

$$F_{mag} = \sum_{i=1}^4 (F_{mag_i}) \geq 60.8 * 4 = 243.2(N).$$

More details in the robots design and first prototype are shown in Fig. 6 and Fig. 7.

Regarding moving on steel surfaces, there are problems needed to be addressed in order to maintain stability of the robot which are sliding and turn-over failure as illustrated in Fig. 8.

1) *Sliding Failure Investigation:* In general case, the robot should be able to climb on different degree of inclination surface as shown in Fig. 9.

Where P is the total weight, \vec{F}_{mag} is the magnetic adhesion force, N is the reaction force, μ is the frictional coefficient and α is the degree of inclination.

Denote that $\sum \vec{F}$ is the total force applied to the robot and F_x and F_y are the force's projected components to x and y axes as shown in Fig. 9. According to Newton's Second Law of Motion, when the robot stops

$$\sum \vec{F} = \vec{0}.$$

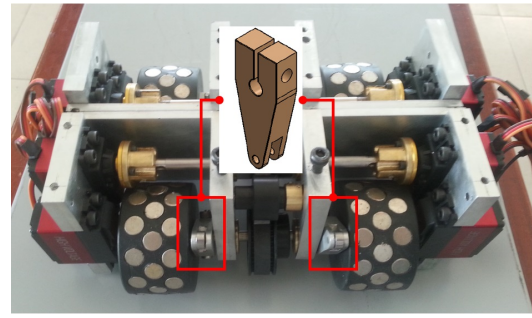


Fig. 4. Two out of four shafts used to lift the robot.

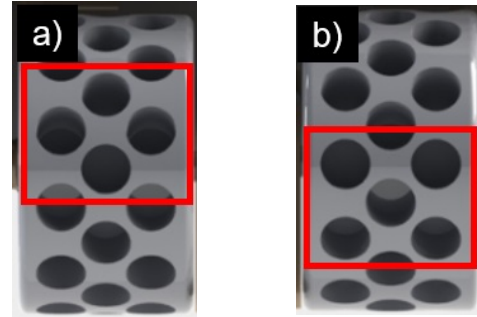


Fig. 5. Wheel design with magnet cylinders.

When the robot is on top of inclined surface as shown in Fig. 9.a:

$$\sum F_y = P \cos \alpha + F_{mag} - N = 0 \Leftrightarrow N = P \cos \alpha + F_{mag}$$

$$\sum F_x = P \sin \alpha - \mu N = 0 \Leftrightarrow N = \frac{P \sin \alpha}{\mu}$$

$$P \cos \alpha + F_{mag} = \frac{P \sin \alpha}{\mu} \Leftrightarrow F_{mag} = \frac{\mu}{\mu} \frac{P \sin \alpha}{\mu} - P \cos \alpha.$$

Therefore, magnetic force should satisfy following condition to avoid sliding failure

$$F_{mag} > \frac{P \sin \alpha}{\mu} - P \cos \alpha. \quad (1)$$

In case the robot moves on bottom of inclined surface as presented in Fig. 9.b:

$$\sum F_y = P \cos \alpha - F_{mag} + N = 0 \Leftrightarrow N = F_{mag} - P \cos \alpha$$

$$\sum F_x = P \sin \alpha - \mu N = 0 \Leftrightarrow N = \frac{P \sin \alpha}{\mu}$$

$$F_{mag} - P \cos \alpha = \frac{P \sin \alpha}{\mu} \Leftrightarrow F_{mag} = \frac{\mu}{\mu} \frac{P \sin \alpha}{\mu} + P \cos \alpha.$$

Therefore, magnetic force should satisfy

$$F_{mag} > \frac{P \sin \alpha}{\mu} + P \cos \alpha. \quad (2)$$

In special case when robot moves on a vertical surface ($\alpha = 90^\circ$)

$$F_{mag} > \frac{P}{\mu}. \quad (3)$$

In general, in order to avoid sliding failure, the value of magnetic force should satisfy

$$F_{mag} > \max \left\{ \frac{P \sin \alpha}{\mu} - P \cos \alpha; \frac{P}{\mu}; \frac{P \sin \alpha}{\mu} + P \cos \alpha \right\}. \quad (4)$$

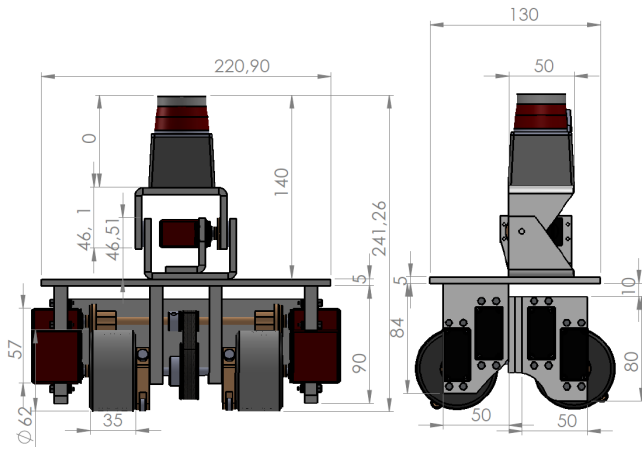


Fig. 6. Robots design in 2D views (unit in millimeter).

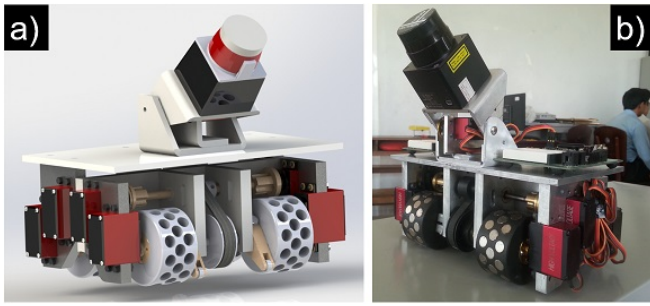


Fig. 7. a) Robot's 3D design; b) Initial prototype of the robot.

Note that:

$$0 < \alpha \leq 90 \Rightarrow \cos \alpha \geq 0. \quad (5)$$

Therefore, the overall condition to avoid sliding failure is

$$F_{mag} > \frac{P \sin \alpha}{\mu} + P \cos \alpha. \quad (6)$$

From the inequality (6), in case magnetic force is a constant value, either decreasing robot weight or increasing frictional coefficient can result in lowering the minimum requirement of sliding avoidance.

Assume the frictional coefficient μ between four wheels and steel surfaces is between 0.5 and 0.8, we notice that $\left(\frac{\sin \alpha}{\mu} + \cos \alpha\right)$ decreases when μ increases and:

$$\begin{aligned} 0.5 < \mu < 0.8; 0 < \alpha \leq 90 \\ \Rightarrow \max \left\{ \frac{\sin \alpha}{\mu} + \cos \alpha \right\} &\approx 2.2361 \\ \Rightarrow F_{mag} &\geq 2.237P. \end{aligned} \quad (7)$$

In conclusion, the magnetic force created by permanent magnets should be at least 2.237 as much as the weight of the robot.

2) *Turn-over Failure Investigation:* From Fig. 10, given L as the distance between front and rear wheels, and d as the distance between the center of mass to steel surface. Moment

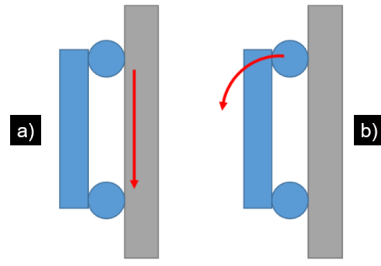


Fig. 8. a) Sliding failure; b) Turn-over failure.

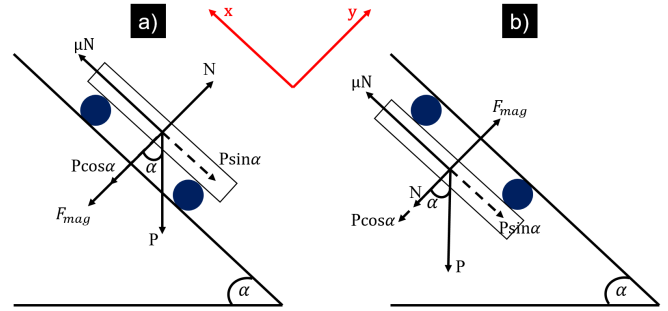


Fig. 9. a) Robot moves on top of inclined surface; b) Robot moves on bottom of inclined surface.

about point A is calculated as follow

$$\sum M = P * d - \frac{F_{mag}}{2} * L \Leftrightarrow F_{mag} = 2 \frac{Pd}{L}.$$

To avoid turn-over failure:

$$F_{mag} > 2 \frac{Pd}{L}. \quad (8)$$

When magnetic force is constant, we can avoid the failure by lowering $\frac{d}{l}$ which means making the robots center of mass closer to the steel surface.

In general, we can avoid sliding and turn-over failure if the magnetic force satisfies

$$F_{mag} > \max \left\{ \frac{P \sin \alpha}{\mu} + P \cos \alpha; 2 \frac{Pd}{L} \right\}. \quad (9)$$

B. Sensor Integration

Fig. 11 presents multiple imaging sensors equipped on robot: a video camera for images capturing and video streaming, a Hokuyo laser scanner, and a time-of-flight camera from MESA for capturing depth images which can be processed later for 3D map construction.

Apart from cameras, eight Hall Effect sensors which are able to detect the presence of magnetic field are also used. Fig. 12 illustrates the sensor's mounting as we use two sensors which are mounted next to each other and close to one wheel. By taking advantage of the fact that magnet cylinders inside each wheel will move when the robot moves, we can extract the velocity and traveling distance of each wheel after combining the data from these two sensors.

In order to provide another input for robot's localization, an Inertial Measurement Unit (IMU) is used in order to help the robot localize itself among the space. According to [26],

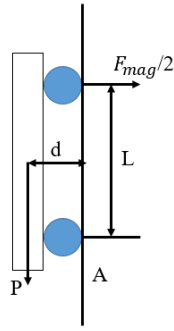


Fig. 10. Moment calculation about point A.



Fig. 11. a) USB Camera; b) Hokuyo Laser Scanner; c) MESA depth camera.

some parameters of the 3DM-GX3-25 IMU are described in Table IV

Besides, the robot has four IR range sensors mounted at four corners of the robot, which can detect whether there is steel surface underneath. Consequently, an edge avoidance algorithm can be implemented using this input to make sure that the robot can safely travel on steel surfaces. Table V shows some features of the IR range sensor [27].

III. ROBOT CONTROL

The robot is controlled by two controllers: a microcontroller (MCU) based controller handling low-level tasks and a more powerful onboard computer for complex processing and communication with ground station. The low-level controller has the capability of receiving commands from onboard computer via serial connection including motion control, sensors data acquisition. The onboard computer is a NUC Core i3 computer from Intel which is responsible

TABLE IV
3DM-GX3-25 IMU PARAMETERS

Attitude heading range	360° about all 3 axes
Static accuracy	±0.5° pitch, roll, heading
Dynamic accuracy	±2.0° pitch, roll, heading
Long term drift	Eliminated
Data output rate	up to 1000 Hz

TABLE V
IR RANGE SENSOR PARAMETERS

Type	Sharp GP2Y0A41SK0F
Distance measuring range	4 cm to 30 cm (1.5 to 12)
Output type	Analog voltage
Update period	16.5 ± 4 milliseconds

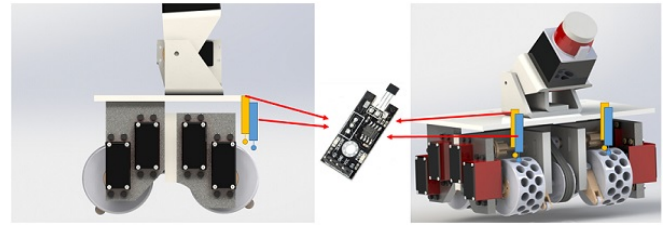


Fig. 12. Hall Effect sensors mount.

for getting video camera and 3D camera images then send them to ground station over wireless LAN connection for data post processing and logging. It also executes the edge avoidance algorithm with sensors data received from the low-level controller to ensure safe traveling on steel surfaces.

Overall, the structure of the system is shown in Fig. 13 and the whole robot is depicted in Fig. 14.

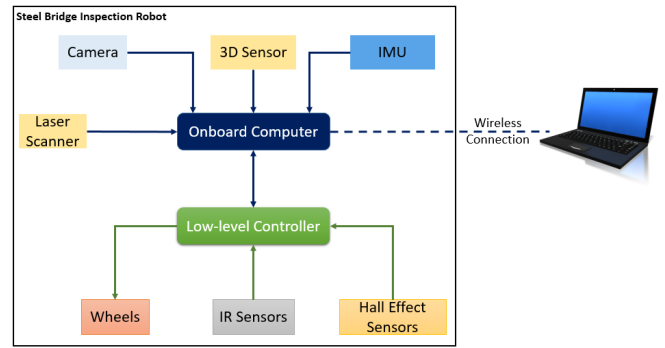


Fig. 13. System architecture.

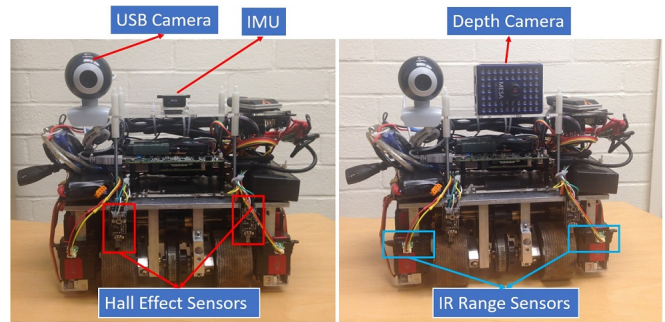


Fig. 14. Robot prototype with integrated sensors.

While moving on steel surfaces, there can be a circumstance that the robot moves far away toward the edge of the surface which it can fall off. Therefore, an algorithm using input from IR range sensors is incorporated to prevent this failure. Denote $dr_i (i = 1, \dots, 4)$ as the calibrated ranges before robot starts moving, $r_i (i = 1, \dots, 4)$ as sensor reading corresponding to $sensor_i$ and $d_i (i = 1, \dots, 4)$ as travel distances calculated from Hall Effect sensors. When sensor reading is out of the range between $[dr_i - \epsilon; dr_i + \epsilon]$ where ϵ is a predefined threshold, the robot considers that there is no steel surface below $sensor_i$.

Algorithm 1: EDGE AVOIDANCE.

Input: $(dr_1, dr_2, dr_3, dr_4), (r_1, r_2, r_3, r_4), \epsilon,$
 (d_1, d_2, d_3, d_4)

```
1 for  $i:=1,4$  do
2   if only one  $(r_i) \notin [dr_i - \epsilon; dr_i + \epsilon]$  then
3     if  $i:=$  front right IR sensor then
4       Stop
5       Go backward with a distance of 5 cm
        ( $\Delta d_i \approx 3$ )
6       Rotate left when travel distance of either
        right wheel reach 3 cm ( $\Delta d_i \approx 2$ )
7       Keep moving
8     Check other sensors and take similar actions
9   else
10    stop and wait for commands
```

IV. EXPERIMENTAL RESULTS

In order to verify the design and assess the performance of the robot, physical experiments were conducted. The tests were under lab environment on built steel bar structures. The ability of climbing and failure avoidance were evaluated under both experiments. During the test, one 2S1P (2 cells) 7.4V 5000 milliampere-hour (mAh) and one 3S1P 11.1V 5000 mAh batteries are used to power the robot. One laptop which can connect to a wireless LAN is used as a ground station.



Fig. 15. Robot can adhere to steel surfaces in different situations.

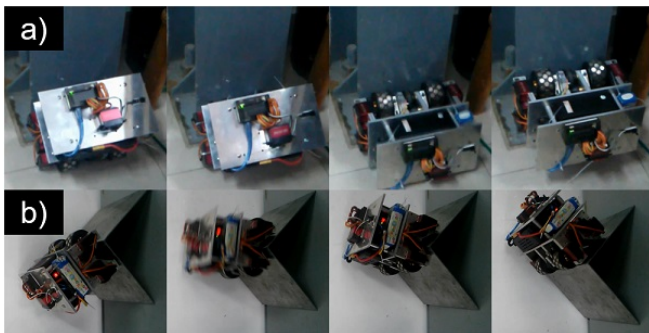


Fig. 16. Surface transition experiments: a) Transitions from ground to steel bar; b) Passes a 90° angle obstacle.

Fig. 15 presents various cases when the robot was placed on steel surfaces under different degrees of inclination to ensure that the magnetic force is strong enough to adhere to steel surfaces when the robot does not move. In all cases, the robot showed strong adhesion force without sliding or turn-over failure.

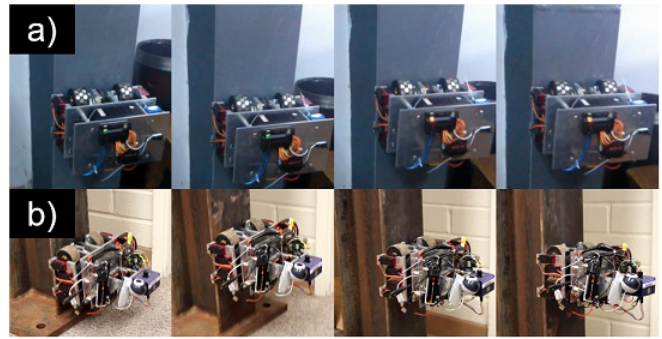


Fig. 17. Robot moves on steel surfaces: a) Without load; b) Full load.

The surface transition ability was also validated in two cases: 1) Robot started from the ground (horizontal plane) and climbed on a steel bar (vertical plane); 2) Robot passed a right angle obstacle. Eventually, the robot successfully went through both cases as illustrated in Fig. 16.

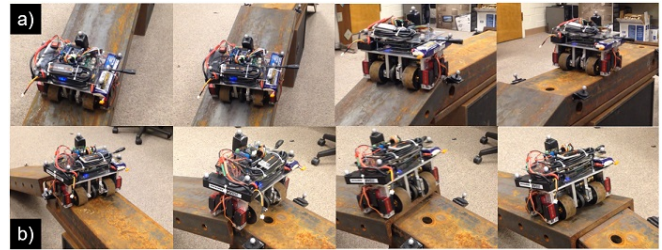


Fig. 18. Robot moves on a bridge-like steel structure with Edge Avoidance algorithm validation.

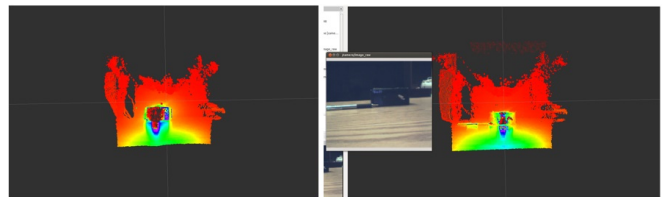


Fig. 19. a) Depth image; b) Visual image versus depth image.

Moreover, robot is also capable of vertically moves on steel surface as shown in Fig. 17 when the robot has no load and full load. The velocity of the robot is approximately 10 centimeters/second. In another test, the robot moves on a constructed steel structures from one end to the other end. The robot successfully reaches the destination as well as using lifting mechanism to overcome stuck condition as shown in Fig. 18.

During the test, data collected from both video camera and depth camera are transmitted over wireless connection to the laptop acting as ground station. Received data are illustrated in Fig. 19.

V. CONCLUSION AND FUTURE WORK

This work describes the design and implementation of a steel climbing robot which is capable of carrying multiple sensors for steel bridge inspection. Initial prototype is implemented and validated to ensure the robot is able to strongly adhere on steel surfaces in multiple situations. The robot is

also able to transition from different surfaces with different inclination levels. There are several sensors attached on the robots while the collected data are transferred to ground station for further process. Moreover, various sensors are integrated to assist the robot's navigation and localization process.

One important step needed to be done is robot localization under steel structures. An approach using visual-inertial odometry is being investigated to support robot autonomous navigation and mapping purposes. Furthermore, implementation of map construction method and on-line visual crack detection algorithm [28], [29] are also within our interest based on our recent result [30]. Additionally, a cooperative process will be investigated to employ multiple robots for inspecting a large steel bridge efficiently in which cooperative control-learning-sensing can be applied [31]–[33].

ACKNOWLEDGMENT

The authors would like to thank Sy. N. Dang, Anh Q. Pham, Anh H. Vo and Quang H. Dinh from Duy Tan University, Vietnam, for their help and support of the robot implementation.

REFERENCES

- [1] U.S. Department of Transportation Federal Highway Administration. National bridge inventory data. <http://www.fhwa.dot.gov/bridge/nbi.cfm>.
- [2] Minnesota Department of Transportation. I-35w st. anthony falls bridge collapse. <http://www.dot.state.mn.us/i35wbridge/collapse.html>.
- [3] N. Gucunski, S. H. Kee, H. M. La, B. Basily, A. Maher, and H. Ghasemi. Implementation of a fully autonomous platform for assessment of concrete bridge decks. *Structures Congress, Portland, Oregon, USA*, pages 367–378, 2015.
- [4] H. M. La, N. Gucunski, S. H. Kee, J. Yi, T. Senlet, and L. Nguyen. Autonomous robotic system for bridge deck data collection and analysis. *IEEE Inter. Conf. on Intelligent Robots and Systems (IROS), Chicago, Illinois, USA*, pages 1950–1955, 2014.
- [5] H. M. La, R. S. Lim, B. B. Basily, N. Gucunski, J. Yi, A. Maher, F. A. Romero, and H. Parvardeh. Autonomous robotic system for high-efficiency non-destructive bridge deck inspection and evaluation. *IEEE Inter. Conf. on Auto. Sci. and Eng. (CASE), Madison, Wisconsin, USA*, pages 1065–1070, 2013.
- [6] J.E. DeVault. Robotic system for underwater inspection of bridge piers. *Instrumentation Measurement Magazine, IEEE*, 3(3):32–37, Sep 2000.
- [7] R. S. Lim, H. M. La, Z. Shan, and W. Sheng. Developing a crack inspection robot for bridge maintenance. *IEEE Inter. Conf. on Robotics and Automation (ICRA), Shanghai, China*, pages 6288–6293, 2011.
- [8] R. S. Lim, H. M. La, and W. Sheng. A robotic crack inspection and mapping system for bridge deck maintenance. *IEEE Trans. on Automation Science and Engineering*, 11(2):367–378, April 2014.
- [9] H.M. La, R.S. Lim, B.B. Basily, N. Gucunski, Jingang Yi, A. Maher, F.A. Romero, and H. Parvardeh. Mechatronic systems design for an autonomous robotic system for high-efficiency bridge deck inspection and evaluation. *Mechatronics, IEEE/ASME Transactions on*, 18(6):1655–1664, Dec 2013.
- [10] H.M. La, N. Gucunski, S.-H. Kee, and L.V. Nguyen. Data analysis and visualization for the bridge deck inspection and evaluation robotic system. *Visualization in Engineering*, 3(1):1–16, 2015.
- [11] Bing Li, Jing Cao, Jizhong Xiao, Xiaochen Zhang, and Hongfan Wang. Robotic impact-echo non-destructive evaluation based on fft and svm. In *Intelligent Control and Automation (WCICA), 2014 11th World Congress on*, pages 2854–2859, June 2014.
- [12] Fengyu Xu and Xingsong Wang. Design and experiments on a new wheel-based cable climbing robot. In *Advanced Intelligent Mechatronics, 2008. AIM 2008. IEEE/ASME International Conference on*, pages 418–423, July 2008.
- [13] K.H. Cho, H.M. Kim, Y.H. Jin, F. Liu, H. Moon, J.C. Koo, and H. R. Choi. Inspection robot for hanger cable of suspension bridge: Mechanism design and analysis. *Mechatronics, IEEE/ASME Transactions on*, 18(6):1665–1674, Dec 2013.
- [14] Je-Keun Oh, An-Yong Lee, Se Min Oh, Youngjin Choi, Byung-Ju Yi, and Hai Won Yang. Design and control of bridge inspection robot system. In *Mechatronics and Automation, 2007. ICMA 2007. International Conference on*, pages 3634–3639, Aug 2007.
- [15] R.T. Pack, Jr. Christopher, J.L., and K. Kawamura. A rubbertuator-based structure-climbing inspection robot. In *Robotics and Automation, 1997. Proceedings., 1997 IEEE International Conference on*, volume 3, pages 1869–1874 vol.3, Apr 1997.
- [16] M. Abderrahim, C. Balaguer, A. Gimenez, J.M. Pastor, and V.M. Padron. Roma: a climbing robot for inspection operations. In *Robotics and Automation, 1999. Proceedings. 1999 IEEE International Conference on*, volume 3, pages 2303–2308 vol.3, 1999.
- [17] A. Mazumdar and H.H. Asada. Mag-foot: A steel bridge inspection robot. In *Intelligent Robots and Systems, 2009. IROS 2009. IEEE/RSJ International Conference on*, pages 1691–1696, Oct 2009.
- [18] Rui Wang and Y. Kawamura. A magnetic climbing robot for steel bridge inspection. In *Intelligent Control and Automation (WCICA), 2014 11th World Congress on*, pages 3303–3308, June 2014.
- [19] Quancai Liu and Yong Liu. An approach for auto bridge inspection based on climbing robot. In *Robotics and Biomimetics (ROBIO), 2013 IEEE International Conference on*, pages 2581–2586, Dec 2013.
- [20] Yong Liu, Qifan Dai, and Quancai Liu. Adhesion-adaptive control of a novel bridge-climbing robot. In *Cyber Technology in Automation, Control and Intelligent Systems (CYBER), 2013 IEEE 3rd Annual International Conference on*, pages 102–107, May 2013.
- [21] A. Leibbrandt, G. Caprari, U. Angst, R.Y. Siegwart, R.J. Flatt, and B. Elsener. Climbing robot for corrosion monitoring of reinforced concrete structures. In *Applied Robotics for the Power Industry (CARPI), 2012 2nd International Conference on*, pages 10–15, Sept 2012.
- [22] H. Leon-Rodriguez, S. Hussain, and T. Sattar. A compact wall-climbing and surface adaptation robot for non-destructive testing. In *Control, Automation and Systems (ICCAS), 2012 12th International Conference on*, pages 404–409, Oct 2012.
- [23] A. San-Millan. Design of a teleoperated wall climbing robot for oil tank inspection. In *Control and Automation (MED), 2015 23th Mediterranean Conference on*, pages 255–261, June 2015.
- [24] Dapeng Zhu, Jiajie Guo, Chunhee Cho, Yang Wang, and Kok-Meng Lee. Wireless mobile sensor network for the system identification of a space frame bridge. *Mechatronics, IEEE/ASME Transactions on*, 17(3):499–507, June 2012.
- [25] Inc K&J Magnetics. Original magnet calculator. <https://www.kjmagnetics.com/>.
- [26] MicroStrain. 3dm-gx3-25 imu. <http://www.microstrain.com/>.
- [27] Sharp. GP2Y0A41SK0F IR rangefinder. <http://www.sharp-world.com/>.
- [28] T. H. Dinh, Q. P. Ha, and H. M. La. Computer vision-based method for concrete crack detection. In *Proceedings of the 14th International Conference on Control, Automation, Robotics and Vision (ICARCV), November 13-15, 2016, Phuket, Thailand.*, pages 1–7, 2016.
- [29] P. Prasanna, K. J. Dana, N. Gucunski, B. B. Basily, H. M. La, R. S. Lim, and H. Parvardeh. Automated crack detection on concrete bridges. *IEEE Transactions on Automation Science and Engineering*, 13(2):591–599, April 2016.
- [30] N.H. Pham, H.M. La, Q.P. Ha, S.N. Dang, A.H. Vo, and Q.H. Dinh. Visual and 3d mapping for steel bridge inspection using a climbing robot. In *The 33rd International Symposium on Automation and Robotics in Construction and Mining (ISARC)*, pages 141–149, July 2016.
- [31] H. M. La and W. Sheng. Distributed sensor fusion for scalar field mapping using mobile sensor networks. *IEEE Trans. on Cybernetics*, 43(2):766–778, Apr. 2013.
- [32] H. M. La, W. Sheng, and J. Chen. Cooperative and active sensing in mobile sensor networks for scalar field mapping. *IEEE Trans. on Systems, Man and Cybernetics, Part A: Systems*, 45(1):1–12, Jan. 2015.
- [33] H. M. La, R. Lim, and W. Sheng. Multi-robot cooperative learning for predator avoidance. *IEEE Trans. on Control Systems Technology*, 23(1):52–63, Jan 2015.